NeuroImage: Clinical 26 (2020) 102205

Contents lists available at ScienceDirect

NeuroImage: Clinical

journal homepage: www.elsevier.com/locate/ynicl

Somatosensory evoked fields predict response to vagus nerve stimulation

Karim Mithani[a,1], Simeon M. Wong[b,1], Mirriam Mikhail[a], Haatef Pourmotabbed[c,e], Elizabeth Pang[f], Roy Sharma[f], Ivanna Yau[f], Ayako Ochi[f], Hiroshi Otsubo[f], O. Carter Snead[f,g], Elizabeth Donner[f], Cristina Go[f], Elysa Widjaja[g,h], Abbas Babajani-Feremi[c,d,e], George M. Ibrahim[b,g,i,*]

[a] Faculty of Medicine, University of Toronto, Toronto, Canada
[b] Institute of Biomaterials and Biomedical Engineering, University of Toronto, Toronto, Canada
[c] Department of Pediatrics, University of Tennessee Health Science Center, Memphis, TN, USA
[d] Department of Anatomy and Neurobiology, University of Tennessee Health Science Center, Memphis, TN, USA
[e] Neuroscience Institute, Le Bonheur Children's Hospital, Memphis, TN, USA
[f] Division of Neurology, Hospital for Sick Children, Toronto, Canada
[g] Institute of Medical Science, University of Toronto, Toronto, Canada
[h] Department of Diagnostic Imaging, Hospital for Sick Children, Toronto, Canada
[i] Division of Neurosurgery, Hospital for Sick Children, Department of Surgery, University of Toronto, Toronto, Canada

ARTICLE INFO

Keywords:
Connectomics
Evoked potentials
Machine learning
SEF
VNS

ABSTRACT

There is an unmet need to develop robust predictive algorithms to preoperatively identify pediatric epilepsy patients who will respond to vagus nerve stimulation (VNS). Given the similarity in the neural circuitry between vagus and median nerve afferent projections to the primary somatosensory cortex, the current study hypothesized that median nerve somatosensory evoked field(s) (SEFs) could be used to predict seizure response to VNS. Retrospective data from forty-eight pediatric patients who underwent VNS at two different institutions were used in this study. Thirty-six patients ("Discovery Cohort") underwent preoperative electrical median nerve stimulation during magnetoencephalography (MEG) recordings and 12 patients ("Validation Cohort") underwent preoperative pneumatic stimulation during MEG. SEFs and their spatial deviation, waveform amplitude and latency, and event-related connectivity were calculated for all patients. A support vector machine (SVM) classifier was trained on the Discovery Cohort to differentiate responders from non-responders based on these input features and tested on the Validation Cohort by comparing the model-predicted response to VNS to the known response. We found that responders to VNS had significantly more widespread SEF localization and greater functional connectivity within limbic and sensorimotor networks in response to median nerve stimulation. No difference in SEF amplitude or latencies was observed between the two cohorts. The SVM classifier demonstrated 88.9% accuracy (0.93 area under the receiver operator characteristics curve) on cross-validation, which decreased to 67% in the Validation cohort. By leveraging overlapping neural circuitry, we found that median nerve SEF characteristics and functional connectivity could identify responders to VNS.

1. Introduction

Epilepsy is the most common serious neurological condition of childhood, affecting 1-2% of the pediatric population (Hauser et al., 1991; Russ et al., 2012). Up to 40% of these children do not respond to anti-seizure drug therapy, and may benefit from surgical management (Chen et al., 2018; Devinsky, 1999; Kwan and Brodie, 2000). Vagus nerve stimulation (VNS) is a safe and well-tolerated treatment option for drug-resistant epilepsy that involves modulation of vagus nerve activity through an implantable stimulator.

Although VNS is generally effective and widely used, patient outcomes are heterogeneous. Studies have shown that 26% to 55% of children undergoing VNS will respond to stimulation, which is defined as >50% reduction in seizure frequency (Klinkenberg et al., 2012; Terra et al., 2014). The inability to preoperatively identify responders from non-responders may subject some children to the risks of surgery

* Corresponding author at: Division of Neurosurgery, Hospital for Sick Children, 555 University Avenue, Room 1503, Toronto, ON, Canada, M5G 1X8
E-mail address: george.ibrahim@sickkids.ca (G.M. Ibrahim).
[1] Co-first authors as they contributed equally to this work.

https://doi.org/10.1016/j.nicl.2020.102205
Received 12 November 2019; Received in revised form 2 February 2020; Accepted 3 February 2020
Available online 04 February 2020

without the subsequent benefits, and in circumstances where resources are limited, precludes children who might benefit from receiving the therapy. The identification of relevant biomarkers to predict seizure response to therapy is increasingly needed.

Recent studies have shown that patient stratification on the basis of brain connectomics and enabled by machine learning algorithms is superior to clinical covariates (Babajani-Feremi et al., 2018; Ibrahim et al., 2017; Mithani et al., 2019). Specifically, evaluation of preoperative neuronal connectivity between brain regions within the Vagus Afferent Network (VagAN) has been shown to robustly predict outcomes following VNS (Ibrahim et al., 2017; Mithani et al., 2019). The VagAN has been recently described to encompass the afferent projections of the vagus nerve via brainstem pathways to the thalamus and cortex (Hachem et al., 2018).

One of the regions of the VagAN is the primary somatosensory cortex. The vagus nerve carries general somatic afferent (GSA), general visceral afferent (GVA) and efferent fibres. The majority of the fibres of the vagus nerve are comprised of GVA (Rutecki, 1990). Vagal afferents to the visceral region of the primary somatosensory cortex have been widely reported and preserved across species (Ito, 2002; Ito and Craig, 2003).

A robust method to evaluate the somatosensory cortex is through median nerve stimulation. Although sensory afferents of the median nerve ascend and decussate within the spinothalamic tract, there is substantial overlap with vagus afferent circuitry at the thalamic level (Fig. 1). Median nerve fibres travel rostrally to synapse in several thalamic nuclei, including the ventral-posterolateral (VPL) nucleus. In comparison, afferents of the vagus nerve project primarily to the nucleus tractus solitarius (NTS) and parabrachial nuclei, and subsequently to the ventral-posteromedial (VPM) nucleus of the thalamus. After synapsing in their respective thalamic nuclei, nerves from both the median and vagus nerves course through the corona radiata to their respective topographic targets within the primary somatosensory cortex (S1). Given these shared afferent pathways, an assessment of the organization, activation, and connectivity of the somatosensory cortex through median nerve stimulation could serve as a model to understand the effects of VNS on neural circuitry and potentially seizure responsiveness.

In the current study, the overlapping neural circuitry between median and vagus nerve afferents was leveraged to predict seizure responsiveness to VNS. Specifically, we hypothesized that – given the common afferent neuronal circuits shared by the median and vagus nerves – features of median nerve stimulation could serve as a surrogate for evaluating electrophysiological characteristics of the vagus afferent network. Following this, we further hypothesized that certain qualities of somatosensory evoked fields recorded through magnetoencephalography (MEG) could in fact predict response to VNS. MEG provides unbiased localization of the S1 and can sample large-scale brain networks with high-fidelity temporal resolution and reasonable spatial resolution (Bardouille et al., 2018). Median nerve stimulation could therefore be applied as a means to pre-operatively interrogate some of the electrophysiological features of the vagus afferent network. Features of SEFs that were used to distinguish responders and non-responders included spatial deviation, amplitude and latency, and event-related connectivity. The results of this work provide evidence of the use of SEFs for preoperative prediction of outcomes following VNS and the utility of exploiting overlapping neural circuitry to understand unrelated neurological phenomena.

2. Methods

2.1. Subjects

Retrospective data from 48 consecutively recruited patients was collected from two centres; 36 patients from The Hospital for Sick Children (Toronto, Canada) (the “Discovery Cohort”) and 12 from LeBonheur Children's Hospital (Memphis, Tennessee) (the “Validation Cohort”). Patients in the Discovery Cohort underwent VNS implantation between the years 2000 and 2016 for medically refractory epilepsy and preoperatively underwent median nerve stimulation with concurrent MEG to localize the SEFs. Of these participants, twenty-six were VNS responders (defined as >50% reduction in seizure frequency) and

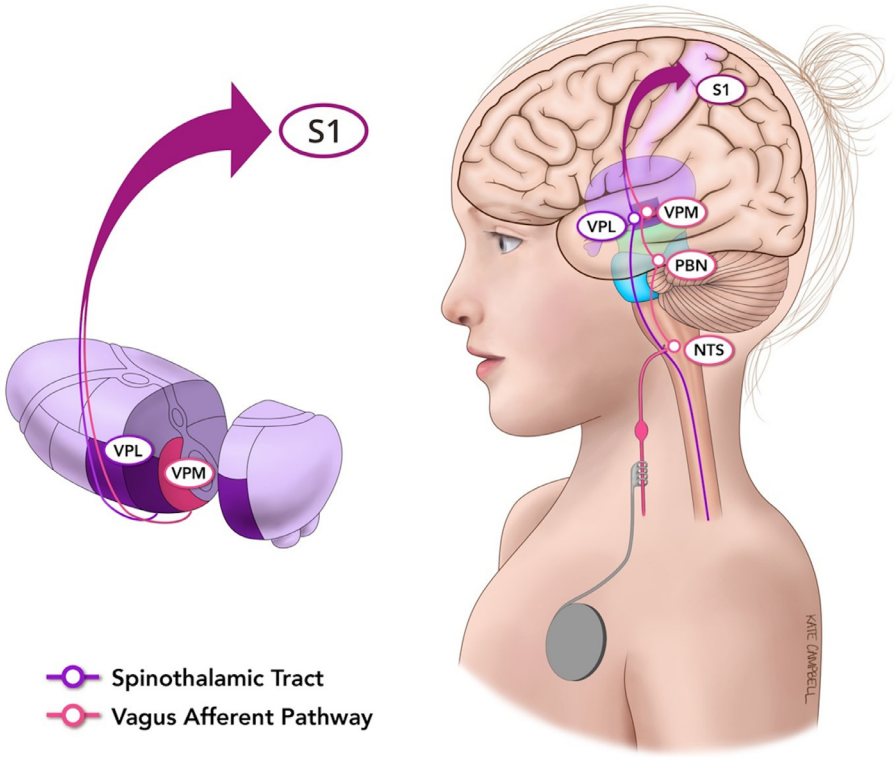

Fig. 1. Median and vagus nerve afferent projections to the primary somatosensory cortex. Median nerve fibres travel rostrally to synapse in several thalamic nuclei, including the ventral-posterolateral (VPL) nucleus. In comparison, afferents of the vagus nerve project primarily to the nucleus tractus solitarius (NTS) and parabrachial nuclei, and subsequently to the ventral-posteromedial (VPM) nucleus of the thalamus. After synapsing in their respective thalamic nuclei, nerves from both the median and vagus nerves course through the corona radiata to their respective topographic targets within the primary somatosensory cortex (S1).

Table 1
Overview of clinical characteristics for the Discovery Cohort.

Clinical variable	Responders (*N* = 26)	Non-responders (*N* = 10)	P-value
Sex	Male: 16 (62%) Female: 10 (38%)	Male: 4 (40%) Female: 6 (60%)	0.39
Age	14.7	13.7	0.21
Length of follow-up	1.79	2.29	0.25
Handedness	Right: 20 (77%) Left: 4 (15%) Ambi: 2 (8%)	Right: 7 (70%) Left: 2 (20%) Ambi: 1 (10%)	0.82
Epilepsy duration	7.13	7.91	0.33
Developmental delay	11 (42%)	4 (40%)	0.92
Generalized seizures	14 (54%)	6 (60%)	0.71
Previous resective surgery	3 (12%)	1 (10%)	1.00

No significant difference were found between responders and non-responders for any of these key clinical variables. P-values were generated with either Student's independent samples t-test (for continuous variables) or Fisher's exact test (for discrete variables).

ten were non-responders. For all patients, response was determined after no further benefit from VNS was observed by the treating team after optimal programming parameters were set. All notes from neurosurgeons, neurologists, nurses, and nurse practitioners were reviewed to determined outcome. No discrepancies were identified in the rates of seizure reduction that changed the final classification of any participant's outcome.

Demographic information for the Discovery Cohort is provided in Table 1. There were no significant differences in age, sex, or length of follow-up between VNS responders and non-responders. Patients in the Validation Cohort underwent VNS implantation between the years of 2011 and 2016 for drug-resistant epilepsy and preoperatively underwent pneumatic stimulation with concurrent MEG to localize SEFs. In this cohort, 6 patients were responders and 6 non-responders. Demographic information for this cohort is provided in Table 2.

This study was reviewed and approved by the Hospital for Sick Children Research Ethics Board and by the Institutional Review Board of the University of Tennessee Health Science Center.

2.2. MEG acquisition and pre-processing

Patients within the Discovery Cohort underwent routine clinical median nerve stimulation with concurrent 151-channel clinical CTF MEG (CTF MEG International, Coquitlam, BC), as previously described (Doesburg et al., 2013; Sharma et al., 2007). The clinical indication for median nerve stimulation was to pre-surgically map the primary somatosensory cortex. A Grass Stimulator was used to stimulate the median nerve at each wrist for each patient (rate: 5.1 Hz; duration: 2.1μsec). A total of 400 trials was recorded, with a trial length of 200 ms and a 50 ms pre-trigger interval. Each SEF trial was replicated during collection and data sets with motion >5 mm were discarded. During these stimulations, MEG was acquired at a sampling rate of 2500 Hz with an online low-pass anti-aliasing filter at 625 Hz. Recordings with excessive artefacts or motion were repeated.

Table 2
Overview of clinical characteristics for the Validation Cohort.

Clinical variable	Responders (N = 6)	Non-responders N = 6)	P-value
Sex	Male: 2 (33%) Female: 4 (67%)	Male: 2 (33%) Female: 4 (67%)	1.00
Age (mean ± SD year)	9.2 ± 6.6	13.5 ± 10.3	0.41
Length of follow-up (mean ± SD year)	3.4 ± 2.1	2.0 ± 0.9	0.21
Handedness	Right: 4 (67%) Left: 1 (17%) Ambi: 1 (17%)	Right: 5 (83%) Left: 1 (17%) Ambi: 0 (0%)	1.00
Epilepsy duration (mean ± SD year)	4.9 ± 2.5	7.4 ± 4.7	0.27
Developmental delay	4 (67%)	3 (50%)	1.00
Generalized seizures	2 (33%)	2 (33%)	1.00
Previous resective surgery	0 (0%)	2 (33%)	0.45

As part of the routine clinical procedure used at Le Bonheur Children's hospital, patients within the Validation Cohort underwent pneumatic stimulation during MEG recordings, as previously described (Castillo et al., 2004). MEG data were recorded with a sampling rate of 508.63 or 678.17 Hz using a whole-head magnetometer containing 248 sensors (WH 3600, 4D Neuroimaging). The somatosensory stimuli were delivered via pneumatically driven mechanical taps that were applied to the distal fingertips of the subject's right or left index finger via a balloon diaphragm. The right or left index finger received 400 stimuli with an inter stimulus interval of 550 ± 50 ms. All analyses were performed in MATLAB R2018a software (Mathworks Inc., Natick, MA), using the FieldTrip toolbox (Oostenveld et al., 2011).

2.3. Localization of SEFs

MEG data were epoched and averaged during median nerve stimulation. Epochs were windowed from -50 ms to 150 ms relative to the stimulus onset. The data were bandpass filtered from 1 to 150 Hz with a 4th order two-pass Butterworth filter and were notch filtered at 60 Hz. An equivalent current dipole (ECD) method was used to localize the generator of the first major neuromagnetic peak following stimulation. This method produces an anterior facing dipole that accurately localizes the primary somatosensory cortex. We used the ECD method to localize the primary somatosensory cortex in both hemispheres by stimulating the contralateral arm and to obtain the latency of the functional response of the somatosensory cortex (peak of the first component). Patients with SEF coordinates greater than three standard deviations from the mean were excluded from analysis. This included five subjects in total: three with outliers on the right only, and two with outliers on both the left and the right. Three of these outliers were VNS responders and two were non-responders, leaving a total of twenty-three VNS responders and eight non-responders in the Discovery Cohort.

2.4. Construction of whole brain connectomes

Broadband (1-150 Hz) time series representing activity from the primary somatosensory cortex as well as 128 cortical and subcortical seed locations representing the Desikan-Killiany (DK) atlas (Desikan et al., 2006) were constructed. Briefly, the DK atlas coordinates were unwarped from standard Montreal Neurological Institute (MNI) space into each patients's brain space using SPM8 normalization functions. Vector beamforming was used to reconstruct broadband time series representing activity from these 128 regions following median nerve or pneumatic stimulation. Source time series were estimated by applying the linearly constrained minimum variance (LCMV) beamformer, using a subject-specific single shell head model.

2.5. Spatial deviation of SEFs maximal activation

The spatial deviation of each patient's SEFs from a reference point was calculated. The point of reference consisted of the coordinates of the primary somatosensory cortex from the DK atlas: x = -43 mm, y = -23 mm, and z = 49 mm on the left, and x = 40 mm, y = -25 mm, z = 53 mm on the right. Spatial deviation was defined as the Euclidean distance between the point of maximal activation of the SEF in standard space and the aforementioned, corresponding reference point and calculated using Eq. (1), where "*i*" indicates coordinates for each individual and "*s*" indicates the standard reference coordinate from the DK atlas.

$$D = \sqrt{(x_i - x_S)^2 + (y_i - y_S)^2 + (z_i - z_S)^2}$$

2.6. Latency and amplitude of SEFs

SEF peaks, including N20, P25, and N45, were visually marked by a trained observer and cross-referenced between both beamformed data and unprocessed sensor recordings. Data peaks were independently verified by two authors (K.M. and G.M.I.). The corresponding latencies and amplitudes were extracted from the beamformed data. For the right hemisphere, only 30 patients were analyzed (22 responders, 8 non-responders) due to a technical issue with left median nerve stimulation. Thirty-one patients (23 responders, 8 non-responders) were included with left hemisphere data. The spatial deviation of the SEFs as well as the amplitudes and latencies were compared between groups using the Student's t-test.

2.7. Functional connectivity analysis

After pre-processing and source reconstruction, MEG time series data were filtered into alpha (8–14 Hz), beta (15–24 Hz), and low gamma (25–35 Hz) frequency bands. Time resolved power spectra were computed using the short-time Fourier transform (80 ms Hamming window with 60 ms overlap). Phase synchronization between regions of the DK during median nerve stimulation was calculated using the weighted phase lag index (wPLI) (Vinck et al., 2011) and averaged across trials.

To identify differences in neural network connectivity following median nerve stimulation between VNS responders and non-responders, connectivity matrices were generated for each subject. Matrices were 128 × 128 with each element representing the wPLI values between the various regions of the DK atlas at each frequency. Differences in bandlimited functional connectivity were assessed using the Network Based Statistics (NBS) toolbox (Zalesky et al., 2012). NBS first independently tests the hypothesis of interest at each analyzed connection (edge) and then generates sets of edges that exceed the user-specified test statistical threshold ($t \geq 2.5$). Topographical clusters of contiguous suprathreshold connections are then identified and assigned a family-wise error rate (FWER)-corrected *p*-value using permutation testing with 5000 permutations. Significant network differences between responders and non-responders at each frequency were visualized using the BrainNet Viewer Toolbox (Xia et al., 2013).

2.8. Support vector machine learning

Support vector machines (SVMs) are a type of supervised models that involve building a binary linear classifier for a particular outcome using a labelled training dataset (Hearst et al., 1998). A SVM was trained using the Discovery Cohort for classification of responders and non-responders to VNS. The following features were included in the model: the spatial deviation of the SEFs, the amplitude and latencies of the reconstructed SEFs in each hemisphere, and the functional connectivity data. In order to avoid overfitting the data, only the wPLI value between the homologous somatosensory cortices was extracted from the connectivity matrices and entered into the training model. This was chosen as all significant networks demonstrated this homologous connection using NBS. A receiver operating characteristic (ROC) curve was plotted to illustrate the classification ability of the model at varying discrimination thresholds. The SVM classifiers were generated using the MATLAB Statistics and Machine Learning Toolbox (9.3.0, R2017b).

2.9. Classifier validation

A completely independent sample of patients from a second institution (i.e. the Validation Cohort) was then used to validate the model. The Validation Cohort underwent preoperative pneumatic sensory stimulation to identify the SEFs. All MEG recordings were pre-processed in the same manner as the Discovery Cohort. The SVM classifier was applied to the test cohort to predict their response to VNS, and then compared to their known percentage change in main seizure reduction. The final classifier as a MATLAB *ClassificationSVM* model object is available upon request.

3. Results

3.1. Subjects

The twenty-six VNS responders exhibited a mean seizure reduction of 98.3% (standard deviation [SD] 2.99%), whereas the non-responders demonstrated a mean seizure reduction of 32.4% (SD 50.3%). The median seizure reduction was 85.7%, and a total of 11 patients (35%) achieved seizure freedom. Seizure outcomes were assessed over an average of 2.01 years (median 1.60 years, range: 0.2 – 6.7 years). No statistically significant association were identified between patient covariates and VNS responsiveness (Table 1).

3.2. Maximal activation of SEFs

The average Euclidean distance between the point of SEF maximal activation and reference S1 for all subjects was 13.2 ± 7.7 mm and 15.7 ± 11.5 mm with left and right-sided stimulation, respectively (Fig. 2; Table 3). Responders exhibited a mean SEF deviation of

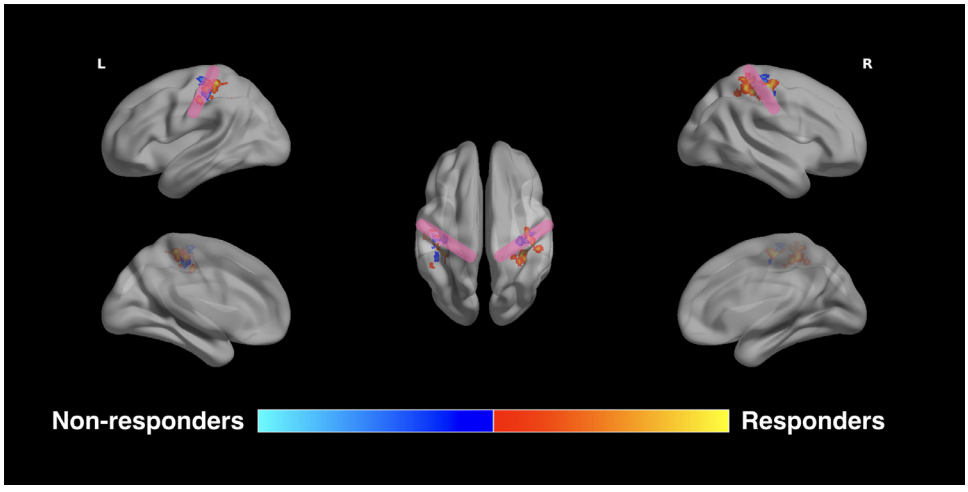

Fig. 2. Spatial deviation of somatosensory evoked fields. VNS responders exhibit a greater distance between the primary somatosensory cortex and the point of maximum activation of their somatosensory evoked fields. This increased spatial deviation is statistically significant with right-sided stimulation ($p = 0.0003$), but not left-sided stimulation ($p = 0.059$).

Table 3
Group differences in the spatial distribution of maximal SEF activation between VNS responders and non-responders.

Side of SEF activation	Group	Mean Euclidean Distance (mm)	p-value*
Right	Responders	15.18	0.0003
	Non-responders	6.43	
Left	Responders	14.31	0.059
	Non-responders	9.97	

* Based on Student's *t*-test (2-tailed).

14.3 ± 6.7 mm and 15.1 ± 7.2mm with left and right median nerve stimulation, respectively, whereas non-responders had deviations of 10 ± 4.6mm and 6.4 ± 4mm, respectively. The SEF deviation between the point of maximal activation and the reference coordinates for S1 was significantly greater in VNS responders than non-responders with right-sided stimulation (Student's t-test, $n = 31$, $p = 0.0003$), but not left-sided stimulation (Student's t-test, $n = 31$, $p = 0.059$) (Fig. 2).

3.3. Latency and amplitude of SEFs in VNS responders vs. non-responders

Three standard peaks were averaged, identified and analyzed for each SEF recording for each patient (Table 4). These included the N20, P25, and N45. VNS non-responders exhibited a mean latency of 0.020s, 0.026s and 0.044s for the N20, P25 and N45 peaks, respectively. There were no differences identified based on laterality. In contrast, VNS responders had a mean latency of 0.019s, 0.25s, 0.042s/0.043s for the N20, P25 and Left/Right N45 peaks, respectively. The shorter latencies identified in the VNS responders did not reach the threshold for statistical significance (Student's t-test, $n = 31$, $p > 0.05$). The amplitudes of each of the peaks was also computed and compared between responders and non-responders to VNS. No significant differences were identified (Student's t-test, $n = 31$, Table 5; $p > 0.05$).

3.4. Functional connectivity associated with VNS response

Event-related functional connectivity was computed and NBS was used to determine significant differences between responders and non-responders. Network functional connectivity at the main event-related peak was significantly greater in responders compared to non-responders in the beta (15–24 Hz) and gamma (25–40 Hz) bands. In the beta band (with right median stimulation), the most significant connectivity differences were identified in frontal and limbic circuitry, whereas gamma band differences (with left median stimulation) were dominated by greater connectivity within the sensorimotor network in VNS responders (Fig. 3; 5000 permutations, $n = 31$, FWER-corrected $p < 0.05$).

3.5. Support vector machine learning to predict VNS response

SEF characteristics and functional connectivity (confined to the S1 nodes bilaterally to avoid overfitting) were used as input dimensions in the SVM. The algorithm demonstrated an accuracy of 88.9% (95% specificity, 67% sensitivity) with an area under the ROC curve (AUC) of 0.93 on 10-fold cross-validation.

Upon external validation performed using the Validation Cohort, our classifier was able to correctly predict response to VNS implantation in 8 out of 12 patients, with an accuracy of 67%, a sensitivity of 83%, and a specificity of 50%.

Table 4
Group differences in the latencies of key SEF peaks between VNS responders and non-responders.

Side of SEF activation	Peak	Mean Latency (Non-responders)	Mean Latency (Responders)	p-value*
Right	N20	0.0195	0.0193	0.88
	P25	0.0260	0.0258	0.88
	N45	0.0442	0.0430	0.43
Left	N20	0.0197	0.0185	0.13
	P25	0.0260	0.0243	0.09
	N45	0.0438	0.0418	0.06

* Based on Student's *t*-test (2-tailed).

Table 5
Group differences in the amplitudes of key SEF peaks between VNS responders and non-responders.

Side of SEF activation	Peak	Mean Amplitude (Non-responders)	Mean Amplitude (Responders)	p-value*
Right	N20	0.753	12.67	0.33
	P25	0.669	4.44	0.34
	N45	0.481	6.12	0.34
Left	N20	0.902	0.770	0.59
	P25	0.922	2.31	0.50
	N45	0.262	1.63	0.32

* Based on Student's *t*-test (2-tailed).

4. Discussion

Although VNS is increasingly used to treat medically-intractable epilepsy in children, heterogeneity in patient outcomes poses a challenge. There is a need to accurately identify children preoperatively who will benefit from surgery, while sparing those who may not benefit the potential surgical risks. Here, we leveraged similarities in the afferent projections of the median and vagus nerves to the primary somatosensory cortex to develop a predictive algorithm to VNS, with three main findings. First, spatial deviation of the point of maximal activation of SEFs, but not their amplitude and latency, is associated with VNS responsiveness. Second, significant event-related differences in functional connectivity within limbic and sensorimotor networks are present between responders and non-responders. Third, a predictive algorithm based on SVM learning was able to accurately predict VNS responders. This algorithm performed well on cross-validation with lower accuracy in an external cohort with a modification of the SEF technique, utilizing pneumatic stimulation rather than electrical stimulation of the median nerve. These findings expand our understanding of the mechanism of action of VNS and provide support for the use of overlapping neural circuitry within the VagAN to predict responsiveness to VNS.

4.1. Leveraging overlapping circuitry to overcome challenges in assessment of vagus afferents

The current study leveraged similarity in circuitry between vagus and median nerve afferents to deduce meaningful insights into the afferent vagus circuitry. During surgical implantation of VNS, Usami and colleagues recorded scalp evoked potentials from the vagus nerve using clinically-relevant stimulation parameters (Usami et al., 2013). These evoked potentials persisted despite muscular blockade, suggesting that they were not attributable to the electromyogram of pharyngeal muscles induced by descending impulses. Historically, however, direct evoked potentials from the vagus nerve were rather difficult to record (Hammond et al., 1992; Tougas et al., 1993). Furthermore, such responses to vagus stimulation at the time of surgery cannot be utilized as presurgical tools to direct preoperative treatment decisions. Alternative methods, such as evoked potentials recorded during transcutaneous stimulation of the vagus nerve are in their infancy (Nonis et al., 2017) and biased by muscular contamination and efferent effects that are difficult to disentangle (Polak et al., 2014). The use of median nerve SEFs as a model for VNS impulse supplies novel opportunities to study

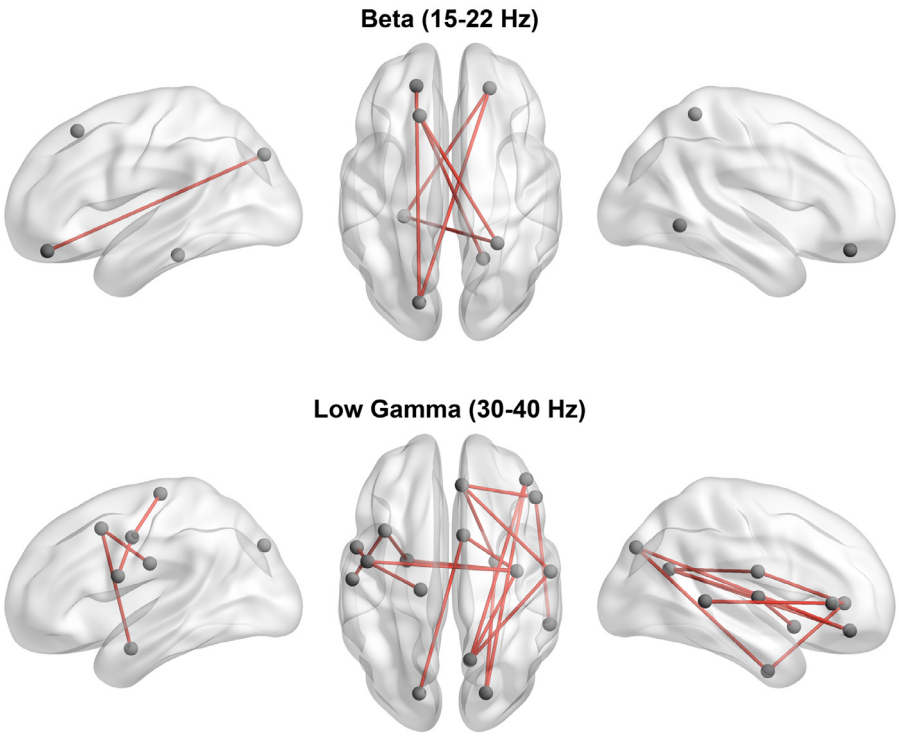

Fig. 3. Event-related connectivity differences between responders and non-responders. Responders to VNS demonstrate significantly greater event-related connectivity in limbic and sensorimotor circuitry in the beta and gamma bands, respectively.

the VagAN and stratify patients by treatment response.

4.2. VNS responders exhibit a greater spatial extent of SEFs than non-responders

We speculate that when the SEF demonstrates significantly greater spatial deviation (relative to a reference point for the primary somatosensory cortex), thalamocortical afferent projections of the median nerve to the S1 are more widespread. Extrapolating these findings to vagus afferents suggests that VNS may modulate a wider network, potentially resulting in greater efficacy. Direct projections from the vagus nerve to the thalami have been reported (Beckstead et al., 1980) and early electrophysiological studies in animals have demonstrated widespread electrocorticographic changes consistent with thalamic modulation with VNS (Chase et al., 1966). In humans, VNS stimulation has been associated with increases in blood flow in the thalamus and cingulate cortex (Henry et al., 1999, 2004; Ko et al., 1996). Data from event-related functional MRI studies also support a role for activation of the thalamus, basal ganglia and insular cortices with active stimulation (Narayanan et al., 2002), which may be linked to seizure response (Liu et al., 2003). A wider network of activation, as implied by our median nerve SEF findings, could result in an ability to modulate cortical excitability over larger areas, and therefore greater seizure responsiveness.

4.3. Event-related functional connectivity associated with VNS response

Using a whole-brain connectomic approach, we also defined event-related functional changes occurring following median nerve stimulation. Children who responded to VNS demonstrated significantly greater connectivity within limbic and motor networks with median nerve stimulation, respectively. It is possible that physiological conduction blocks in the afferent brainstem and thalamic pathways prevent non-responders from modulating large-scale networks in response to median nerve stimulation. Indeed, dysfunction of brainstem and thalamic afferent circuitry has been suggested by recent studies evaluating cardiac autonomic function in patients undergoing VNS. Cardiovascular autonomic dysregulation, indexed by heart rate variability, is caused by brainstem lesions (Monge Argilés et al., 2000) and thalamocortical dysfunction (Chang et al., 2013; Mueller et al., 2019) and has been found to be associated with response to VNS (Liu et al., 2017).

The findings of impairments in the sensorimotor networks in the gamma band are noteworthy. Intrinsic connectivity (resting-state) networks have been reported in MEG across multiple frequencies (Brookes et al., 2011; Hipp et al., 2012). In a recent study of directed connectivity in MEG, Gao and colleagues investigated Granger causality during evoked responses elicited by air puff stimulation of the index finger (Gao et al., 2015). They found interhemispheric connectivity from the primary S1 to secondary ipsilateral and contralateral regions. More robust connectivity in responders may represent more efficient information flow across these large-scale networks. The limbic circuitry being more strongly connected in responders in the beta band may represent intrinsic connections that are facilitated in this cohort (Mithani et al., 2019).

4.4. The vagus afferent network and treatment response

We have previously shown that the brain's resting intrinsic connectivity within the VagAN may predict response to VNS (Babajani-Feremi et al., 2018; Ibrahim et al., 2017; Mithani et al., 2019). The VagAN represents the afferent neural circuitry that is modulated by VNS, which may be further understood through the study of brain connectomics to inform surgical candidacy (Hachem et al., 2018). Critical regions of the VagAN that have been related to treatment response include limbic, thalamocortical and association fibres (Ibrahim et al., 2017; Mithani et al., 2019).

The primary somatosensory cortex is one of the few regions of the VagAN that could be probed through activation studies in the form of evoked potentials. In the current work, a linear SVM classifier generated using SEF characteristics and connectivity differed significantly between responders and non-responders, demonstrating robust internal validity in predicting response to VNS, with an AUC of 0.93 and

accuracy of 88.9%. The accuracy decreased to 67% when generalized to a model utilizing pneumatic hand stimulation. These findings further support the concept of brain network mapping within the VagAN to predict seizure response to VNS.

4.5. Limitations and future directions

The current work presents a novel, multi-institutional approach, exploiting overlapping brain circuitry to probe critical brain regions implicated in afferent VNS circuitry. These analyses, involving a limited number of participants with retrospectively collected data provide a basis for a larger scale study. Although there is substantial heterogeneity in the current population, we have shown in these analyses and in previous studies (Mithani et al., 2019) that clinical covariates are not strongly predictive of treatment response. Age is an important consideration and is known to affect SEF amplitudes and latencies, which, interestingly, were the only characteristics of the SEF which did not differ significantly between responders and non-responders. Finally, the trained model was only moderately generalizable to the Validation Cohort, which underwent a different paradigm to elicit SEFs in MEG than the Discovery Cohort. Although sensitivity was relatively high, the overall accuracy was substantially lower at 67%. It is unclear whether these differences could be exclusively attributed to the different paradigms or modest model generalizability. A large-scale, prospective multicenter project, the Connectivity and Vagus Nerve Stimulation Outcome Study (CONNECTiVOS), is currently underway in North American which may aid in further validating the present findings.

5. Conclusions

By leveraging similarity in neural circuitry between vagus and median nerve afferent projections to the primary somatosensory cortex, we were able to demonstrate that VNS responders may be identified using median nerve SEF in MEG. The spatial extent of the SEF as well as event-related functional connectivity differentiated responders from non-responders in a support vector machine learning model. The current work provides further support for the study of the VagAN through brain network mapping and connectomic methodology to understand the mechanism of action of VNS and preoperatively identify candidates who are likely to benefit from therapy.

Funding

This work was supported by the Canadian Institutes for Health Research Project Grant.

KM, SW, ABF, and **GMI** conceived of the study. **KM, SW, MM, HP,** and **ABF** designed and performed analyses. **KM, EP, RS, IY, AO, HO,** and **ED** wrote the manuscript and drafted figures and tables. **OCS, ED, CG, EW, ABF**, and **GMI** contributed to and reviewed the manuscript.

Declaration of Competing Interest

None

References

Babajani-Feremi, A., Noorizadeh, N., Mudigoudar, B., Wheless, J.W., 2018. Predicting seizure outcome of vagus nerve stimulation using MEG-based network topology. NeuroImage Clin 19, 990–999. https://doi.org/10.1016/j.nicl.2018.06.017.

Bardouille, T., Power, L., Lalancette, M., Bishop, R., Beyea, S., Taylor, M.J., Dunkley, B.T., 2018. Variability and bias between magnetoencephalography systems in non-invasive localization of the primary somatosensory cortex. Clin. Neurol. Neurosurg. 171, 63–69. https://doi.org/10.1016/j.clineuro.2018.05.018.

Beckstead, R.M., Morse, J.R., Norgren, R., 1980. The nucleus of the solitary tract in the monkey: projections to the thalamus and brain stem nuclei. J. Comp. Neurol. 190, 259–282.

Brookes, M.J., Woolrich, M., Luckhoo, H., Price, D., Hale, J.R., Stephenson, M.C., Barnes, G.R., Smith, S.M., Morris, P.G., 2011. Investigating the electrophysiological basis of resting state networks using magnetoencephalography. Proc. Natl. Acad. Sci. U. S. A. 108, 16783–16788. https://doi.org/10.1073/pnas.1112685108.

Castillo, E., Simos, P., Wheless, J., Baumgartner, J., Breier, J., Billingsley, R., Sarkari, S., Fitzgerald, ME, Papanicolaou, A., 2004. Integrating sensory and motor mapping in a comprehensive MEG protocol: clinical validity and replicability. Neuroimage 21, 973–983.

Chang, C., Metzger, C.D., Glover, G.H., Duyn, J.H., Heinze, H.J., Walter, M., 2013. Association between heart rate variability and fluctuations in resting-state functional connectivity. Neuroimage 68, 93–104. https://doi.org/10.1016/j.neuroimage.2012.11.038.

Chase, M.H., Sterman, B., Clemente, C.D., 1966. Cortical and to subcortical afferent vagal patterns stimulation of response. Exp. Neurol. 16, 36–49.

Chen, Z., Brodie, M.J., Liew, D., Kwan, P., 2018. Treatment outcomes in patients with newly diagnosed epilepsy treated with established and new antiepileptic drugs: a 30-year longitudinal cohort study. JAMA Neurol. 75, 279–286. https://doi.org/10.1001/jamaneurol.2017.3949.

Desikan, R.S., Se, F., Fischl, B., Quinn, B.T., Dickerson, B.C., Blacker, D., Buckner, R.L., Dale, A.M., Maguire, R.P., Hyman, B.T., Albert, M.S., Killiany, R.J., 2006. An automated labeling system for subdividing the human cerebral cortex on MRI scans into gyral based regions of interest. Neuroimage 31, 968–980. https://doi.org/10.1016/j.neuroimage.2006.01.021.

Devinsky, O., 1999. Patients with refractory seizures. N. Engl. J. Med. 340, 1565–1570. https://doi.org/10.1056/NEJM199905203402008.

Doesburg, S.M., Ibrahim, G.M., Smith, M.L., Sharma, R., Viljoen, A., Chu, B., Rutka, J.T., 3rd, O.C.S., Pang, E.W., 2013. Altered rolandic gamma-band activation associated with motor impairment and ictal network desynchronization in childhood epilepsy. PLoS One 8, e54943.

Gao, L., Sommerlade, L., Coffman, B., Zhang, T., Stephen, J.M., Li, D., Wang, J., Grebogi, C., Schelter, B., 2015. Granger causal time-dependent source connectivity in the somatosensory network. Sci. Rep. 5, 1–10. https://doi.org/10.1038/srep10399.

Hachem, L.D., Wong, S.M., Ibrahim, G.M., 2018. The vagus afferent network: emerging role in translational connectomics. Neurosurg. Focus 45, 1–8. https://doi.org/10.3171/2018.6.FOCUS18216.

Hammond, E., Uthman, B., Reid, S., Wilder, B., 1992. Electrophysiologic studies of cervical vagus nerve stimulation in humans: II. Evoked potentials. Epilepsia 33, 1021–1028.

Hauser, W.A., Annegers, J.F., Kurland, L.T., 1991. Prevalence of epilepsy in rochester, minnesota: 1940–1980. Epilepsia 32, 429–445. https://doi.org/10.1111/j.1528-1157.1991.tb04675.x.

Hearst, M., Dumais, S., Osuna, E, 1998. Support vector machines. IEEE Intell. Syst. their Appl. 13, 18–28.

Henry, T., Votaw, J., Pennell, P., Epstein, C., Bakay, R., Faber, T., Grafton, S., Hoffman, J., 1999. Acute blood flow changes and efficacy of vagus nerve stimulation in partial epilepsy. Neurology 52, 1166–1173.

Henry, T.R., Bakay, R.A.E., Pennell, P.B., Epstein, C.M., Votaw, J.R., 2004. Brain blood-flow alterations induced by therapeutic vagus nerve stimulation in partial epilepsy: II. Prolonged effects at high and low levels of stimulation. Epilepsia 45, 1064–1070.

Hipp, J.F., Hawellek, D.J., Corbetta, M., Siegel, M., Engel, A.K., 2012. Large-scale cortical correlation structure of spontaneous oscillatory activity. Nat. Neurosci. 15, 884–890. https://doi.org/10.1038/nn.3101.

Ibrahim, G.M., Sharma, P., Hyslop, A., Guillen, M.R., Morgan, B.R., Wong, S., Abel, T.J., Elkaim, L., Cajigas, I., Shah, A.H., Fallah, A., Weil, A.G., Altman, N., Bernal, B., Medina, S., Widjaja, E., Jayakar, P., Ragheb, J., Bhatia, S., 2017. Presurgical thalamocortical connectivity is associated with response to vagus nerve stimulation in children with intractable epilepsy. NeuroImage Clin 16, 634–642. https://doi.org/10.1016/j.nicl.2017.09.015.

Ito, S., 2002. Visceral region in the rat primary somatosensory cortex identified by vagal evoked potential. J. Comp. Neurol. 24, 10–24. https://doi.org/10.1002/cne.10120.

Ito, S.I., Craig, A.D., 2003. Vagal input to lateral area 3a in cat cortex. J. Neurophysiol. 90, 143–154. https://doi.org/10.1152/jn.01054.2002.

Klinkenberg, S., Van Den Bosch, C.N.C.J., Majoie, H.J.M., Aalbers, M.W., Leenen, L., Hendriksen, J., Cornips, E.M.J., Rijkers, K., Vles, J.S.H., Aldenkamp, A.P., 2012. Behavioural and cognitive effects during vagus nerve stimulation in children with intractable epilepsy: a randomized controlled trial. Eur. J. Paediatr. Neurol. 17, 82–90.

Ko, D., Heck, C., Grafton, S., Apuzzo, M., Couldwell, W., Chen, T., Day, J., Zelman, V., Smith, T., DeGiorgio, C., 1996. Vagus nerve stimulation activates central nervous system structures in epileptic patients during PET H215O blood flow imaging. Neurosurgery 39, 426–431.

Kwan, P., Brodie, M.J., 2000. Early identification of refractory epilepsy. N. Engl. J. Med. 342, 314–319. https://doi.org/10.1056/NEJM200002033420503.

Liu, H., Yang, Z., Huang, L., Qu, W., Hao, H., Li, L., 2017. Heart-rate variability indices as predictors of the response to vagus nerve stimulation in patients with drug-resistant epilepsy. Epilepsia 58, 1015–1022. https://doi.org/10.1111/epi.13738.

Liu, W., Mosier, K., Kalnin, A., Marks, D., 2003. BOLD fMRI activation induced by vagus nerve stimulation in seizure patients. J. Neurol. Neurosurg. Psychiatry 74, 811–814.

Mithani, K., Mikhail, M., Morgan, B.R., Wong, S., Weil, A.G., Deschenes, S., Wang, S., Bernal, B., Guillen, M.R., Ochi, A., Otsubo, H., Yau, I., Lo, W., Pang, E., Holowka, S., Mrt, R., Snead, O.C., Donner, E., Rutka, J.T., Go, C., Widjaja, E., Ibrahim, G.M., 2019. Connectomic profiling identifies responders to vagus nerve stimulation 1–11. 10.1002/ana.25574.

Monge Argilés, J., Palacios Ortega, F., Vila Sobrino, J., Bautista Prados, J., Pérez Vicente, J., Morales Ortiz, A., Palao Sánchez, A., 2000. Brainstem lesions decrease heart rate variability. Neurologia 15, 158–163.

Mueller, S.G., Bateman, L.M., Nei, M., Goldman, A.M., Laxer, K.D., 2019. Brainstem atrophy in focal epilepsy destabilizes brainstem-brain interactions: preliminary

findings. NeuroImage Clin. 23. https://doi.org/10.1016/j.nicl.2019.101888.
Narayanan, J.T., Watts, R., Haddad, N., Labar, D.R., Li, P.M., Filippi, C.G., 2002. Cerebral activation during vagus nerve stimulation : a functional MR study. Epilepsia 43, 1509–1514.
Nonis, R., D'Ostilio, K., Schoenen, J., Magis, D., 2017. Evidence of activation of vagal afferents by non-invasive vagus nerve stimulation: an electrophysiological study in healthy volunteers. Cephalalgia 37, 1285–1293. https://doi.org/10.1177/0333102417717470.
Oostenveld, R., Fries, P., Maris, E., Schoffelen, J.M., 2011. FieldTrip: open source software for advanced analysis of MEG, EEG, and invasive electrophysiological data. Comput. Intell. Neurosci. https://doi.org/10.1155/2011/156869. 2011.
Polak, T., Metzger, F.G., Deckert, J., Fallgatter, A.J., 2014. Central neural versus peripheral muscular origin of vagus somatosensory - Evoked potentials. Brain Stimul 7, 624–625. https://doi.org/10.1016/j.brs.2014.04.003.
Russ, S.A., Larson, K., Halfon, N., 2012. A National profile of childhood epilepsy and seizure disorder. Pediatrics 129, 256–264. https://doi.org/10.1542/peds.2010-1371.
Rutecki, P., 1990. Anatomical, physiological, and theoretical basis for the antiepileptic effect of vagus nerve stimulation. Epilepsia 31, S1–S6.
Sharma, R., Panga, E., Mohameda, I., Chu, B., Hunjan, A., Ochi, A., Holowka, S., Gaetz, W., Chuang, S., Snead, O.I., Otsubo, H., 2007. Magnetoencephalography in children: routine clinical protocol for intractable epilepsy at the hospital for sick children. Int. Congr. Ser. 1300, 685–688.
Terra, V.C., Furlanetti, L.L., Nunes, A.A., Thomé, U., Nisyiama, M.A., Sakamoto, A.C., Machado, H.R., 2014. Vagus nerve stimulation in pediatric patients: is it really worthwhile? Epilepsy Behav. 31, 329–333. https://doi.org/10.1016/j.yebeh.2013.10.011.
Tougas, G., Hudoba, P., Fitzpatrick, D., Hunt, R.H., Upton, A.R.M., 1993. Cerebral-evoked potential responses following direct vagal and esophageal electrical stimulation in humans. Am. J. Physiol. - Gastrointest. Liver Physiol. 264. https://doi.org/10.1152/ajpgi.1993.264.3.g486.
Usami, K., Kawai, K., Sonoo, M., Saito, N., 2013. Scalp-recorded evoked potentials as a marker for afferent nerve impulse in clinical vagus nerve stimulation. Brain Stimul 6, 615–623. https://doi.org/10.1016/j.brs.2012.09.007.
Vinck, M., Oostenveld, R., van Wingerden, M., Battaglia, F., Pennartz, C.M.A., 2011. An improved index of phase-synchronization for electrophysiological data in the presence of volume-conduction, noise and sample-size bias. Neuroimage 55, 1548–1565. https://doi.org/10.1016/j.neuroimage.2011.01.055.
Xia, M., Wang, J., He, Y., 2013. BrainNet viewer : a network visualization tool for human brain connectomics. PLoS Med 8, e68910.
Zalesky, A., Cocchi, L., Fornito, A., Murray, M.M., Bullmore, E., 2012. Connectivity differences in brain networks. Neuroimage 60, 1055–1062. https://doi.org/10.1016/j.neuroimage.2012.01.068.